# Rotational Bands in the Doubly Magic Nucleus 56Ni

Rudolph, Dirk; Baktash, C.; Brinkman, M. J.; Caurier, E.; Dean, D. J.; Devlin, M.; Dobaczewski, J.; Heenen, P. H.; Jin, H. Q.; LaFosse, D. R.; Nazarewicz, W.; Nowacki, F.; Poves, A.; Riedinger, L. L.; Sarantites, D. G.; Satula, W.; Yu, C. H.

*Published in:*
Physical Review Letters

*DOI:*
10.1103/PhysRevLett.82.3763

Published: 1999-01-01

# Rotational Bands in the Doubly Magic Nucleus $^{56}$Ni

D. Rudolph,[1] C. Baktash,[2] M. J. Brinkman,[2] E. Caurier,[3] D. J. Dean,[2,6] M. Devlin,[4] J. Dobaczewski,[5,6,7] P.-H. Heenen,[8] H.-Q. Jin,[2,*] D. R. LaFosse,[4,†] W. Nazarewicz,[2,5,6] F. Nowacki,[3] A. Poves,[9] L. L. Riedinger,[6] D. G. Sarantites,[4] W. Satuła,[5,6,7] and C.-H. Yu[2]

[1]*Department of Physics, Lund University, S-22100 Lund, Sweden*
[2]*Physics Division, Oak Ridge National Laboratory, Oak Ridge, Tennessee 37831*
[3]*Institut de Recherches Subatomiques, CNRS-IN2P3 et Université Louis Pasteur, F-67037 Strasbourg, France*
[4]*Chemistry Department, Washington University, St. Louis, Missouri 63130*
[5]*Institute of Theoretical Physics, Warsaw University, PL-00681 Warsaw, Poland*
[6]*Department of Physics, University of Tennessee, Knoxville, Tennessee 37996*
[7]*Joint Institute for Heavy Ion Research, Oak Ridge National Laboratory, Oak Ridge, Tennessee 37831*
[8]*Service de Physique Nucléaire Théorique, U.L.B-C.P. 229, B-1050 Brussels, Belgium*
[9]*Departamento de Fisica Teorica, Universidad Autonoma de Madrid, E-28049 Madrid, Spain*

(Received 29 June 1998; revised manuscript received 9 February 1999)

Structures of the medium- to high-spin states in the doubly magic nucleus $^{56}$Ni have been investigated using the reaction $^{28}$Si($^{36}$Ar, $2\alpha$) and the $\gamma$-ray spectrometer Gammasphere in conjunction with the $4\pi$ charged-particle detector array Microball. Two well-deformed rotational bands have been identified. There is evidence that one of the bands, which is identical to a sequence in the odd-odd neighbor $^{58}$Cu, partially decays via proton emission into the ground state of $^{55}$Co. Predictions of extensive large-scale shell-model and cranked Hartree-Fock and Hartree-Fock-Bogolyubov calculations are compared with the experimental data. [S0031-9007(99)09147-4]

PACS numbers: 21.10.Re, 21.60.–n, 23.20.Lv, 27.40.+z

Spectroscopic data from doubly magic nuclei and their nearest neighbors serve as sources and act as constraints on the parameter sets of the nuclear shell model, and, consequently, define the effective nuclear interactions [1]. The nuclei near $^{56}$Ni are of particular interest as they are amenable to different microscopic theoretical treatments while studying the competition between single-particle and collective excitations. The collective states around $^{56}$Ni involve multiparticle multihole excitations across the $N, Z = 28$ shell gap from the $1f_{7/2}$ shell to the $2p_{3/2}$, $1f_{5/2}$, and $2p_{1/2}$ orbits. Excitations to the higher lying $1g_{9/2}$ orbit are necessary to explain the recently observed rotational bands in $^{58}$Cu [2] and $^{62}$Zn [3,4]. At high excitation energies, reaction studies have revealed evidence for hyperdeformed resonances in the $^{56}$Ni compound [5].

Large-scale shell-model calculations in the full $pf$ configuration space have been successfully used to describe the collective structures of $1f_{7/2}$ midshell nuclei [6,7]. The multiparticle multihole states in nuclei near $^{56}$Ni provide an excellent testing ground to confront the nuclear shell model with cluster models [8] and the approaches based on the mean-field theory [2,3,9].

Because of a low Coulomb barrier, proton emission may compete with $\gamma$ decay of excited states of midmass neutron deficient nuclei. In fact, proton radioactivity was first discovered in the decay of the $I^\pi = 19/2^-$ isomeric state in $^{53}$Co [10]. In a recent Letter we presented the first observation of a prompt ($\tau < 3$ ns) decay of a *well-deformed* excited rotational band in $^{58}$Cu via emission of monoenergetic protons into a *spherical* excited state in $^{57}$Ni [2]. Here we report on the observation of two rotational bands in the self-conjugate doubly magic nucleus $^{56}$Ni. While one of the bands may be readily explained with four-particle–four-hole (4p-4h) excitations within the $pf$ space, the second band seems to involve proton and neutron excitations into the $1g_{9/2}$ orbital. It is found to be nearly degenerate with the band in $^{58}$Cu, and partially decays via prompt proton emission into the ground state of $^{55}$Co, hence establishing the first observation of such a decay from an even-even isotope.

Light ion induced reactions have been previously used to study excited states in $^{56}$Ni [1,11]. The yrast line was followed up to 9.4 MeV excitation energy and a tentative spin of $I^\pi = 10^+$ [1]. We investigated excited states in $^{56}$Ni using the heavy-ion fusion reaction $^{28}$Si($^{36}$Ar, $2\alpha$). The 143 MeV $^{36}$Ar beam was provided by the 88-Inch Cyclotron at the Lawrence Berkeley National Laboratory. The target consisted of a 0.42 mg/cm$^2$ layer of 99.1% enriched $^{28}$Si evaporated onto a 0.9 mg/cm$^2$ Ta foil. The 82 Compton-suppressed Ge detectors of the Gammasphere array [12] were used to detect prompt $\gamma$ radiation. The different reaction residues were selected by detecting evaporated charged particles in the $4\pi$ CsI ball Microball [13] and neutrons in 15 liquid scintillator neutron detectors. Details of the experiment can be found in Refs. [2,14]. The partial cross section for $^{56}$Ni was estimated to be only $\sigma_{\rm rel} \approx 0.02\%$ corresponding to some 200 $\mu$b fusion-evaporation cross section.

Coincidence, intensity balance, and summed energy relations were used to deduce the level scheme illustrated in Fig. 1. The previously reported yrast sequence [1] was

  

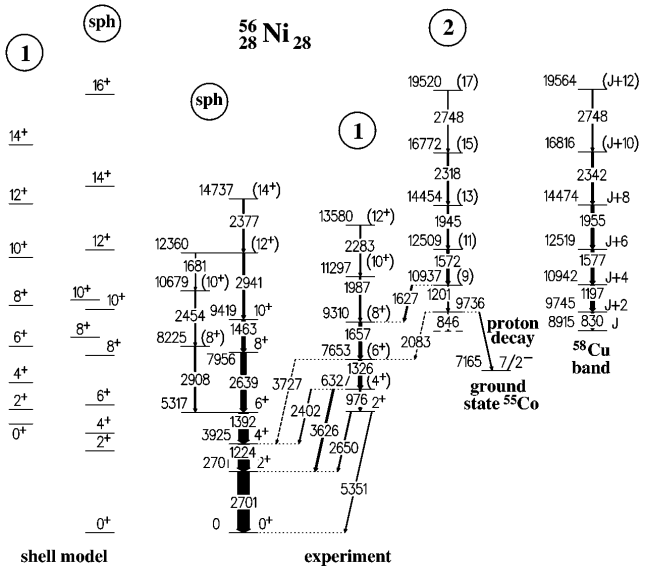


FIG. 1. Proposed partial level schemes of $^{56}$Ni and $^{58}$Cu (right-hand side). The energy labels are given in keV. The widths of the arrows are proportional to the relative intensities of the $\gamma$ rays. Tentative transitions and levels are dashed. On the left-hand side, the energy levels arising from 6p-6h shell-model calculations in the $pf$ model space are shown.

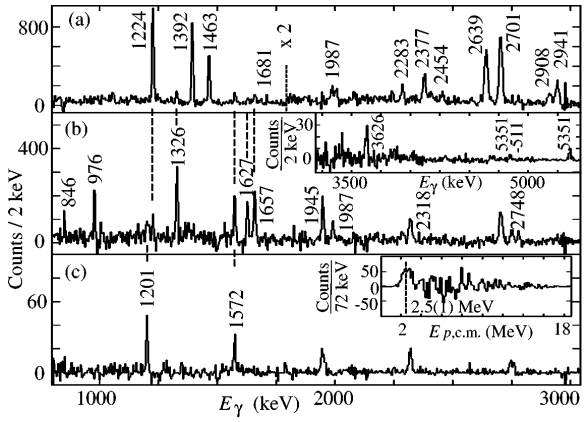


FIG. 2. Gamma-ray spectra of $^{56}$Ni are shown deduced from $\gamma\gamma$ matrices gated by two $\alpha$ particles [(a) and (b)], but asking for one additional proton with $E_{p,\mathrm{c.m.}} \leq 3$ MeV detected in rings 1–4 of Microball (c): Sums of the spectra in coincidence with (a) the known [1] yrast transitions, and (b) members of the rotational bands. The inset of (b) illustrates the high-energy portion of the spectrum. (c) The sum of spectra gated by the 1201, 1572, and 1945 keV transitions. The inset shows the proton center-of-mass energy sum spectrum employing the same $\gamma$-ray gates in a $2\alpha 1p$-gated $E_\gamma$-$E_{p,\mathrm{c.m.}}$ matrix. Peaks are labeled by their energies in keV.

confirmed. In addition, yrare $(8^+)$ and $(10^+)$ states were identified, and the yrast sequence was extended beyond $I = 12\,\hbar$, the maximum possible spin for 2p-2h excitations in the $pf$ shell-model space. Spin and parity assignments are based on directional correlations of oriented states (DCO ratios), angular distributions from singles projections at different Ge-detector angles, and on the regular increase of $\gamma$-ray energies in the rotational bands [14]. Except for the 6327 keV level, our assignments agree with those in Ref. [11]. The angular characteristics for both the 976 and 3626 keV transitions are consistent with a stretched $E2$ radiation [14], and reject the suggested $3^-$ assignment for the 6327 keV level [11].

Figure 2(a) shows the sum of spectra gated with two alphas and the 2701, 1224, 1392, 2639, and 1463 keV transitions that deexcite the spherical states in $^{56}$Ni. Figure 2(b) provides the sum of spectra gated with the 976, 1326, 1572, 1627, and 1657 keV transitions. Next to the transitions in the two rotational bands and the 2701 keV ground-state transition, the high-energy $\gamma$ rays linking the deformed states into the spherical states are clearly visible in the inset of Fig. 2(b). The angular distribution of the 1627 keV interband transition is consistent with that of a stretched dipole. Employing the residual Doppler shift method [15] an average transition quadrupole moment can be estimated for band 2 which is similar to that of the rotational band in $^{58}$Cu($\overline{Q}_t \sim 2\ e\,\mathrm{b}$) [2]. The latter is also displayed in Fig. 1. Further details of the analysis can be found in Refs. [14,16].

Spectra gated with the 1572, 1945, and 2318 keV transitions in band 2 indicate the presence of transitions at 1201 and 846 keV [cf. Fig. 2(b)]. According to their energies, they are likely candidates for the lower-spin band members. The branching ratio of the 1201 keV transition is 34(4)%. Although the 846 keV transition is clearly visible in Fig. 2(b), it is marked tentative because a contamination arising from the ground-state 849 keV transition of the $3\alpha$ evaporation channel $^{52}$Fe cannot be fully excluded. Most interestingly, however, in the spectrum gated with the 1201 keV transition, $\gamma$-decay-out intensity is missing. Summed yields of the (tentative) 846 and 2083 keV transitions, the 1326 and 3727 keV transitions, or the 2701 and 5351 keV ground-state transitions account for only 52(9)% of the yield of the 1572 keV transition. There are three possible explanations: The level at 9736 keV (i) is an isomeric state with $\tau \gtrsim 10$ ns, (ii) decays through several unobserved weak $\gamma$ branches, or (iii) decays via (prompt) proton emission into the ground state of $^{55}$Co. The first explanation is unlikely because the tentative $\gamma$ ray of 846 keV indicates the continuation of band 2 (with a partial half-life of about 1 ps). The second possibility can be ruled out because decays from other low-spin states [11] have not been seen.

As inferred from the masses [17], the binding-energy difference of $^{56}$Ni and $^{55}$Co is 7.165(11) MeV. This implies $Q_p = 2.571(12)$ MeV for the proton branch. However, its verification is more complicated than in the $^{58}$Cu case because of (i) less statistics, (ii) a worse signal to noise ratio (no neutron gating), and (iii) no potential coincidence with $\gamma$ rays in the daughter nucleus (only the ground state of $^{55}$Co can be expected to be populated). To search for evidence of this proton decay, we investigated a $\gamma\gamma$ matrix gated by two $\alpha$ particles and one proton, with and without an additional energy restriction for the

proton ($E_{p,\mathrm{c.m.}} < 3$ MeV). This energy limit reduced the yields of transitions in $\gamma$-gated spectra belonging to the $2\alpha 1p$ channel $^{55}$Co to 4(1)% as compared to the yields deduced from the "nonrestricted" $2\alpha 1p$-gated spectra. However, the yields of transitions of the $^{56}$Ni band 2 remained essentially *unchanged:* 83(15)% are still observed. Figure 2(c) shows the sum of spectra gated by the 1201, 1572, and 1945 keV transitions in the "restricted" $2\alpha 1p$-gated matrix. This spectrum clearly indicates the presence of a prompt proton decay into the *ground state* of $^{55}$Co, because transitions from $^{55}$Co are absent. Because of the mentioned intensity relations, the band cannot have an identical partner in $^{55}$Co either. The inset of Fig. 2(c) illustrates the sum of proton center-of-mass energy spectra in coincidence with the 1201, 1572, and 1945 keV transitions from a $2\alpha 1p$-gated $E_\gamma$ vs $E_{p,\mathrm{c.m.}}$ matrix. Though less evident than $^{58}$Cu [2], there is a peaklike structure visible at 2.5(1) MeV having a FWHM of 0.8(1) MeV. Finally, the ratio $R$ of yields of transitions in the band in spectra gated with the 1201 and 1572 keV transitions in the restricted $2\alpha 1p$- and the $2\alpha$-gated matrices was determined, providing $R = 0.45(7)$ and 0.16(3), respectively. Taking into account the loss of yield by the cut in proton energy, the 78(1)% proton detection efficiency, and the branching ratio of the 1201 keV transition, these numbers are consistent with a 49(14)% proton branch out of the 9736 keV state (cf. Ref. [16]).

A theoretical description of excited states in $^{56}$Ni requires state-of-the-art shell-model and mean-field methods. To understand the spherical states and the deformed band 1, we have carried out the shell-model calculations in the $pf$ shell [18] by allowing the excitation of up to six particles from the $1f_{7/2}$ orbit to the remaining $pf$-shell orbits. The shell-model basis then consists of $25 \times 10^6$ states. As it is discussed in detail in Ref. [19] the KB3 interaction, extensively used in the lower part of the shell, gives a too large quasiparticle gap at the $N, Z = 28$ shell closure. This has been cured by making the diagonal matrix elements which connect the $1f_{7/2}$ orbit with the others 100 keV more attractive. Unfortunately, the $g_{9/2}$ orbit cannot be incorporated easily into the present $pf$ shell-model calculations since it would imply a dramatic increase of the configuration space. Therefore, to describe deformed bands, we employed the cranked Hartree-Fock (HF) [20] and Hartree-Fock-Bogolyubov (HFB) [21] methods with the Skyrme interaction SLy4 [22]. In the HFB calculations, a zero-range density-dependent pairing force has been used, and the particle-number fluctuations have been considered using the Lipkin-Nogami prescription.

The results of the shell-model calculations are plotted on the left-hand side of Fig. 1. The results for the spherical states agree nicely with the observed yrast and yrare states. Also, the predicted $B(E2; 2^+ \rightarrow 0^+) = 130\ e^2\,\mathrm{fm}^4$ agrees well with the experimental value of 120(24) $e^2\,\mathrm{fm}^4$ [23]. (We used the standard isoscalar effective charge $e_\pi + e_\nu = 2$.) Deformed band 1 can be described by both the shell-model and the mean-field calculations. In the shell model it has a dominant 4p-4h character (with respect to the spherical closed core of $^{56}$Ni) and the intrinsic quadrupole moment of 1.3 $e$ b at low spins which becomes $\sim 0.8\ e$ b at $I = 12\,\hbar$. As seen in Figs. 1 and 3(b), the calculated energies agree well with data, although a closer examination indicates that the experimental excitation energies follow the rotational law more closely than the theoretical ones. This can be attributed to the necessary truncation of the shell-model space.

In the mean-field calculations, band 1 can be ascribed to the $4^0 4^0$ configuration with respect to a closed *deformed* core of $^{56}$Ni. Following Refs. [2,14], we label the deformed configurations by the numbers $n$ and $p$ of neutrons and protons occupying the $1g_{9/2}$ $\mathcal{N} = 4$ intruder levels, i.e., $4^n 4^p$. The relevant occupied and empty single-particle Routhians are indicated in Fig. 3(a). At the calculated equilibrium deformations, there appear two large shell gaps at particle numbers 24 and 28. For $^{56}$Ni, the hole states are the $[321]1/2$ and $[312]5/2$ Nilsson orbitals. The first $\mathcal{N} = 4$ orbital, $[440]1/2$, and the $[303]7/2$ extruder level appear just above the $N, Z = 28$ gap. Hence, all the calculated deformed bands in $^{56}$Ni involve *four* $1f_{7/2}$ holes. According to the shell structure of Fig. 3(a), there should be eight bands involving one $\mathcal{N} = 4$ intruder and sixteen $4^1 4^1$ bands. In the following, we concentrate on the lowest bands belonging to these families.

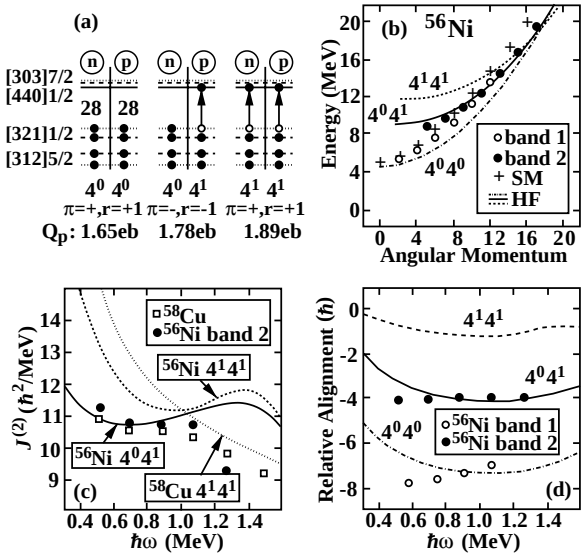


FIG. 3. Properties of deformed bands in $^{56}$Ni according to the cranked HF + SLy4 model. (a) Schematic diagram of single-particle configurations corresponding to the calculated deformed minima (equilibrium quadrupole moments at $\hbar\omega = 1$ MeV are indicated). The $(\pi, r)$ quantum numbers of single-particle Routhians are $(+, -i)$—solid line; $(-, i)$—dotted line; $(-, -i)$—dashed line. (b) Energies of the $4^0 4^0$, $4^0 4^1$, and $4^1 4^1$ bands compared to the shell-model calculations (SM) and experimental bands 1 and 2. (c) Calculated dynamic moments of inertia of bands $4^0 4^1$ and $4^1 4^1$ in $^{56}$Ni and the $4^1 4^1$ band in $^{58}$Cu. (d) Relative alignments, $i_{\mathrm{rel}} \equiv I(^{56}\mathrm{Ni}) - I(^{58}\mathrm{Cu})$, for deformed bands in $^{56}$Ni.

The energies of collective bands in $^{56}$Ni are shown in Fig. 3(b). The band head of the $4^0 4^0$ configuration agrees nicely with the excitation energy of band 1, but its angular momentum alignment is too large. This can be attributed to pairing correlations absent in the HF model. Indeed, in the HFB calculations pairing correlations in this band are large. Unfortunately, they also lead to a spurious mixing between spherical and deformed minima, and the $4^0 4^0$ band becomes unstable with respect to deformation changes in the HFB calculations.

By promoting one particle across the deformed gap from the $[321]1/2(+i)$ to the $[440]1/2$ Routhian, one obtains the $4^1 4^0$ and $4^0 4^1$ bands which have negative parity and odd spins [Fig. 3(a)]. In our calculations, both bands have extremely similar moments of inertia, but the excitation energy of the $4^0 4^1$ structure is lower by 100–200 keV. Their energies agree well with the data [see Fig. 3(b)], and the dynamic moment of inertia, $\mathcal{J}^{(2)}$, shown in Fig. 3(c) for the $4^0 4^1$ band, is consistent with the data up to $\hbar\omega \approx 1.1$ MeV. The maximum in the calculated $\mathcal{J}^{(2)}$ around $\hbar\omega \approx 1.5$ MeV is caused by the crossing between the $[321]1/2$ and $[312]5/2$ Routhians.

By lifting one proton *and* one neutron to the lowest $\mathcal{N} = 4$ level, one obtains the positive-parity even-spin $4^1 4^1$ band which is calculated to lie $\sim$3 MeV above the $4^0 4^1$ band at low and medium spins, but is expected to become yrast at $I > 20\,\hbar$. Its moment of inertia is slightly higher than that of the $4^0 4^1$ configuration; in particular, both bands show the same crossing between the $\mathcal{N} = 3$ Routhians. The crossing is blocked in the $4^1 4^1$ band of $^{58}$Cu as the relevant Routhians are occupied.

Figure 3(d) displays the angular momentum alignment, $i_{\mathrm{rel}}$, for the deformed bands in $^{56}$Ni relative to the deformed band in $^{58}$Cu assuming a band-head spin $J = 9$ for the latter [2]. For the $4^0 4^1$ configuration, the relative alignment is close to $-4$. This is consistent with the angular momentum proposed for band 2. The $4^1 4^1$ band carries $i_{\mathrm{rel}} \approx -0.5$, which is difficult to accommodate experimentally. Therefore, we associate a possibly mixed $4^1 4^0$ and $4^0 4^1$ structure with band 2.

The twinning of band 2 and the band in $^{58}$Cu is difficult to understand theoretically. In particular, in our HF calculations the $\mathcal{J}^{(2)}$ moments of inertia of bands $4^0 4^1$ in $^{56}$Ni and $4^1 4^1$ in $^{58}$Cu differ both at low spins (second $\mathcal{N} = 4$ particle) and at high spins ($\mathcal{N} = 3$ band crossing). The fact that our best theoretical scenario for deformed identical bands in $^{56}$Ni and $^{58}$Cu involves structures with *different* intruder content, is very puzzling and requires further investigations.

To summarize, we have identified two rotational bands in the doubly magic nucleus $^{56}$Ni. Both the extended sequence of spherical states and the first rotational band can be explained by large-scale shell-model calculations in the $pf$ shell. Also the results of cranked mean-field calculations indicate that this band is built primarily upon a 4p-4h excitation *within* the $pf$ shell. The second band, however, is expected to involve particles in the $1g_{9/2}$ orbit, which is supported by its similar behavior to the band in $^{58}$Cu. However, the best scenario for this band is based on one proton promoted to the $1g_{9/2}$ orbit, while a neutron and a proton occupies this orbit in $^{58}$Cu. In addition, a discrete 50% prompt proton decay branch into the ground state of $^{55}$Co in the decay out of the 9736 keV state is observed, constituting the first case of this decay mode in an even-even isotope.

The authors thank LBNL for support. This research was supported by the German BMBF (06-LM-868), the Swedish NSRC, the U.S. DOE [Grants No. DE-FG02-96ER40963 (UT), No. DE-FG05-88ER40406 (WU), and No. DE-FG05-87ER40361 (JIHIR)], the Polish CSR (2 P03B 040 14), the Spanish DGES (PB96-053), the IN2P3(France)-CICYT(Spain) agreements, and NATO (CRG 970196). ORNL is managed by Lockheed Martin Energy Research Corp. for the U.S. DOE under Contract No. DE-AC05-96OR22464.

*Present address: NASA Ames Research Center, Moffett Field, CA 94035.

†Present address: SUNY Stony Brook, Stony Brook, NY 11794.

[1] J. Blomqvist *et al.,* Z. Phys. A **322**, 169 (1985).
[2] D. Rudolph *et al.,* Phys. Rev. Lett. **80**, 3018 (1998).
[3] C. E. Svensson *et al.,* Phys. Rev. Lett. **79**, 1233 (1997).
[4] C. E. Svensson *et al.,* Phys. Rev. Lett. **80**, 2558 (1998).
[5] R. R. Betts, B. B. Back, and B. G. Glagola, Phys. Rev. Lett. **47**, 23 (1981).
[6] S. Lenzi *et al.,* Phys. Rev. C **56**, 1313 (1997).
[7] K. Langanke *et al.,* Phys. Rev. C **52**, 718 (1995).
[8] M. Freer, R. R. Betts, and A. H. Wuosmaa, Nucl. Phys. **A587**, 36 (1995).
[9] E. Caurier *et al.,* Phys. Rev. Lett. **75**, 2466 (1995).
[10] K. P. Jackson *et al.,* Phys. Lett. **33B**, 281 (1970).
[11] J. Huo, Nucl. Data Sheets **67**, 523 (1992).
[12] I.-Y. Lee, Nucl. Phys. **A520**, 641c (1990).
[13] D. G. Sarantites *et al.,* Nucl. Instrum. Methods Phys. Res., Sect. A **381**, 418 (1996).
[14] D. Rudolph *et al.,* Nucl. Phys. **A630**, 417c (1998); Eur. Phys. J. A **4**, 115 (1999).
[15] B. Cederwall *et al.,* Nucl. Instrum. Methods Phys. Res., Sect. A **354**, 591 (1995).
[16] D. Rudolph, in Proceedings of Nuclear Structure '98, edited by C. Baktash (American Institute of Physics, New York, to be published).
[17] G. Audi and A. H. Wapstra, Nucl. Phys. **A565**, 1 (1993).
[18] E. Caurier, shell-model code, Strasbourg, 1990.
[19] G. Martinez-Pinedo *et al.,* Phys. Rev. C **55**, 187 (1997).
[20] J. Dobaczewski and J. Dudek, Comput. Phys. Commun. **102**, 166 (1997); **102**, 183 (1997); (to be published).
[21] P. Bonche, H. Flocard, and P.-H. Heenen, Nucl. Phys. **A598**, 169 (1996).
[22] E. Chabanat *et al.,* Nucl. Phys. **A627**, 710 (1997).
[23] G. Kraus *et al.,* Phys. Rev. Lett. **73**, 1773 (1994).